

# Description of a Laboratory Folded Surface Using Differential Geometry

Ian Mynatt<sup>a</sup>, Stephan Bergbauer<sup>b</sup>, David D. Pollard<sup>a,\*</sup>, Djordje Grujic<sup>c</sup>

<sup>a</sup>Department of Geological and Environmental Sciences, Stanford University, Stanford, CA, 94305

<sup>b</sup>BP Exploration (Alaska) Inc., P.O. Box 196612 Anchorage, Alaska 99519-6612;

<sup>c</sup>Department of Earth Sciences Dalhousie University, Edzell Castle Circle, Halifax NS, B3H 4J1, Canada

\*dpollard@pangea.stanford.edu

## Abstract

By applying differential geometry to analogue models developed by Grujic et al. (2002), we demonstrate that the geometry of such models can be completely and objectively quantified. This quantification then allows for comparison of such models to measured field data and supplants the use of stereonetts to describe and compare 3-D folds. This example supplements and is based on the material found in (Mynatt et al., 2007).

## Generation of the analogue surface

By deforming analogue models made of paraffin wax (e.g. (Grujic, 1993); (Grujic et al., 2002)), it is possible to create intricate 3-D surfaces for comparison with natural fold surfaces. If the model surface resembles the geologic surface, inferences on the sequence and directions of

loading can be drawn for the deformation of the geologic surface from the known boundary conditions of the laboratory model. However, establishing geometric similarity of the model and natural surfaces requires both surfaces to be mapped in three dimensions. Surfaces quantified using differential geometry can be compared precisely for various geometric similarities and differences as a prerequisite for kinematic and dynamic comparisons.

The folded surface considered in this example (Fig. 1) was created by Grujic et al. (2002) for the 3-D visualization of interference patterns of multiply-folded surfaces using an experimental setup described in Grujic (1993). Prior to benchtop deformation, the layer of paraffin wax was shaped approximately like a cylindrical anticline. The deformed surface was scanned in 3-D with sub-millimeter accuracy.

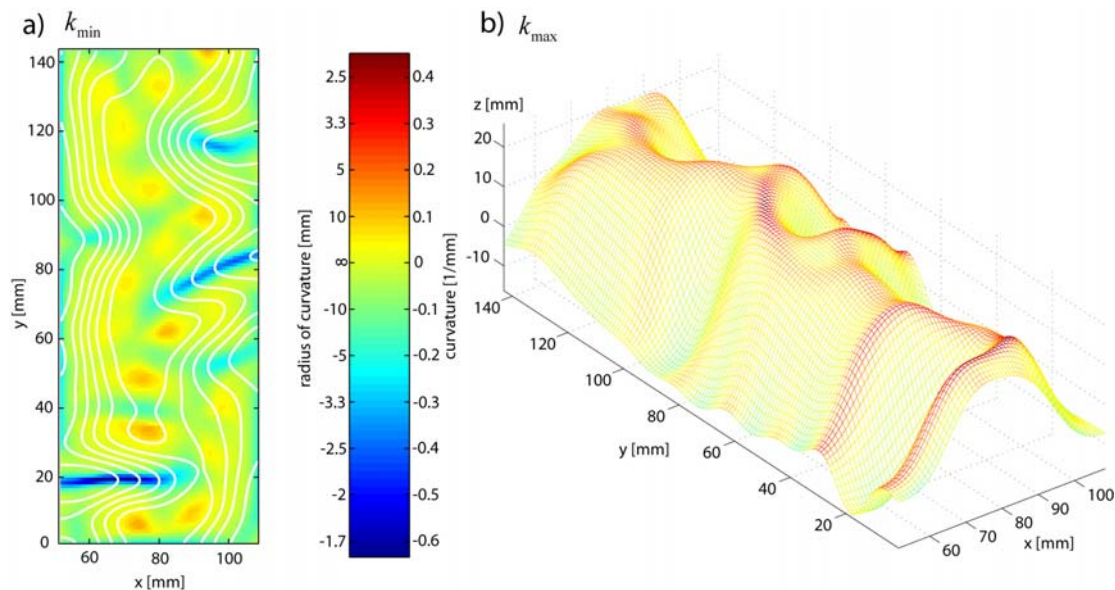


**Figure 1.** Principal curvature magnitudes for analogue model investigating interference patterns of refolded layers (Grujic, 2002). a) Minimum principal curvature,  $k_{\min}$ . White lines are elevation contours. b) Maximum principal curvature,  $k_{\max}$  mapped onto oblique 3-D view of surface.

From the digitized 3-D model, Grujic et al. (2002) chose to produce contoured lower-hemisphere stereographic projections of poles to the surface of the initial fold, and of the refolded layer surface. These contour patterns were then compared to contour patterns from a field example of intricately folded geologic surfaces from the Campolungo area in Switzerland. The authors established a visual match between the contour patterns of analogue models and those from the outcrop data, and inferences on the deformational history of the folded metamorphic terrane were drawn from the known boundary conditions of the laboratory model.





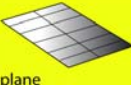



Grujic et al. (2002), however, encountered problems in their attempt to compare fold geometries of the model to those of the metamorphic terrane. These problems are mainly related to the fold description method, which required subjectivity and made locating hinge lines difficult. Also, based on the presence of several closed contours of poles to bedding on stereographic projections, the authors argue for the existence of several cylindrical fold axes when describing non-cylindrical surfaces.

From 984 scanned data points of the analogue surface, we created a numerical 3-D model of the surface with 8,294 equally spaced grid points using cubic interpolation. To remove minor inaccuracies associated with the scanning technique, a spectral filter was applied to the interpolated surface (Bergbauer et al., 2003). Surface undulations with wavelengths smaller than 17 mm were removed. The smoothed surface exhibits a roughly anticlinal shape; however, shortening parallel to the axis of the initial fold resulted in trough and ridge structures (i.e. superposed or second generation folds) that trend at high angles to the initial fold hinge (Fig. 1). Proximity of the loading and constraint platens caused the wax surface to crumple near both ends of the fold. Structures observed in these localities do not contribute to the understanding of folded geologic surfaces and are ignored.

## Geometric analysis of the analogue surface

Visualizations of the analogue fold are obtained using quantities derived from the fundamental forms. Minimum principal curvatures ( $k_{\min}$ ) range from -0.64 to 0.15  $\text{mm}^{-1}$  (Fig. 1a). The maximum principal curvatures ( $k_{\max}$ ) are of the same order of magnitude and range from -0.15 to 0.46  $\text{mm}^{-1}$  (Fig. 1b). Swaths

of nearly constant color depicting extreme magnitudes of  $k_{\min}$  and  $k_{\max}$  trend obliquely to the initial fold hinge, thus highlighting the trends of the hinges of the secondary folds. Hinges associated with the oblique ridge structures merge with the hinge of the initial anticline. Note that all hinges are significantly curved; if these hinges were to be approximated locally by cylindrical folds with straight hinges, their lateral extent would have to be very small, resulting in a large number of fold axes.

	$k_G < 0$	$k_G = 0$	$k_G > 0$
$k_M < 0$	 synformal saddle	 synform	 basin
$k_M = 0$	 perfect saddle	 plane	
$k_M > 0$	 antiformal saddle	 antiform	 dome

**Figure 2. Geologic curvature classification.** The geologic curvature of a point on a surface can be determined from the Gaussian ( $k_G$ ) and mean ( $k_M$ ) curvatures at the point. The color code seen here is used in Figure 3. Modified from (Roberts, 2001) and (Bergbauer, 2002).

Using the concept of geologic curvature (Fig. 2), the model surface can be decomposed into the 8 local surface shapes (Fig. 3). The initial anticlinal structure and the secondary oblique ridge structures are approximated by patches that are shaped like domes and antiformal saddles, whereas the troughs are approximated by basins and synformal saddles (Fig. 3a). The initial structure (i.e. an approximately cylindrical anticline) is obliterated by the small scale undulations of the surface. Transition lines separate each surface shape, and when the curvature threshold ( $k_t$ ) is set to  $1 \times 10^{-3} \text{ mm}^{-1}$ , small areas composed of cylindrical points and perfect saddles emerge near these transition lines (Fig. 3b). Upon setting  $k_t = 1 \times 10^{-2} \text{ mm}^{-1}$ , the fold limbs of the initial anticlinal feature start to emerge as larger areas with contiguous cylindrical shapes (Fig. 3c). With  $k_t = 0.1 \text{ mm}^{-1}$ , parts of the limbs of the initial fold turn into areas of planar points, and the initial hinge is approximated by cylindrical anticlinal points, thereby revealing the original surface shape prior

to the second phase folding (Fig. 3d). The tight trough and ridge structures form synforms and

antiforms that trend obliquely to the hinge of the initial fold.

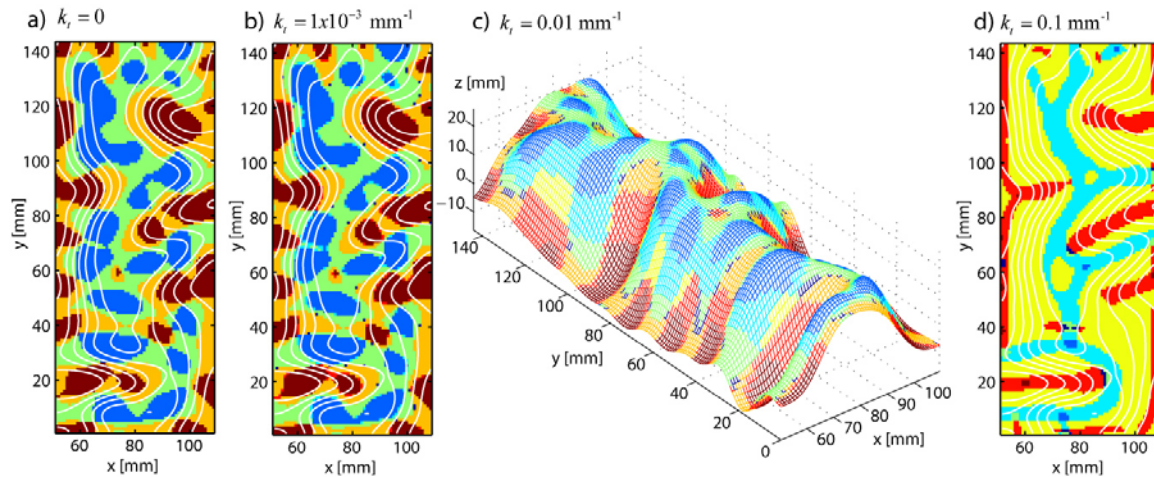


**Figure 3.** Geologic curvature calculations for the analogue model with varying values of the curvature threshold  $k_t$ . Colors indicate the local shape of the surface as indicated in figure 2. Note correlation between antiformal locations and high  $k_{\max}$  areas and synformal areas and high magnitude  $k_{\min}$  areas in figure 1.

## Discussion

While one can construct a stereographic projection of poles to bedding from a given data set of strikes and dips that is unique (e.g. (Grujic et al., 2002)), the construction of a surface from this data set is not unique, because the spatial information has been lost. Possible 3-D surfaces that only honor attitude data might have similar shapes but differ in their fold amplitudes, their closure direction, their length scales, and the number of folds. Thus, representing a folded surface by a stereographic projection of poles to bedding inevitably leads to subjective interpretations of the geometry.

A surface description that is based on the First and Second Fundamental Forms of differential geometry not only is unique, but it is inherently tied to the spatial variations of the surface and does not leave room for a subjective interpretation of the geometry. We thus suggest, particularly for the quantitative comparison of surfaces, that apart from collecting strike and dip measurements of a model or in the field, geologists should record and use the geographic coordinates for every sampled point on the structures they are mapping. Meaningful interpretations of geological surfaces can then be presented quantitatively in light of the sampling, data precision, and motivation of the analysis.

## References

- Bergbauer, S., 2002, The use of curvature for the analysis of folding and fracturing with application to the Emigrant Gap Anticline, Wyoming: Ph. D. thesis, Stanford University, 216 p.
- Bergbauer, S., T. Mukerji, and P. H. Hennings, 2003, Improving curvature analyses of deformed horizons using scale-dependent filtering techniques: American Association of Petroleum Geologist Bulletin.
- Grujic, D., 1993, The influence of initial fold geometry on Type 1 and Type 2 interference patterns: and experimental approach: Journal of Structural Geology, v. 15, p. 293-307.
- Grujic, D., T. R. Walter, and H. Gaertner, 2002, Shape and structure of (analogue models of) refolded layers: Journal of Structural Geology, v. 24.
- Mynatt, I., S. Bergbauer, and D. D. Pollard, 2007, Using differential geometry to describe 3-D folds: Journal of Structural Geology, v. in press.
- Roberts, A., 2001, Curvature attributes and their application to 3D interpreted horizons: First Break, v. 19, p. 85-100.